Quantum Optical Waveform Conversion

D. Kielpinski,[1,3] J. F. Corney,[4] and H. M. Wiseman[2,3]

[1]*ARC Centre of Excellence for Coherent X-Ray Science, Griffith University, Nathan QLD 4111, Australia*
[2]*ARC Centre of Excellence for Quantum Computation and Communication Technology, Griffith University, Nathan QLD 4111, Australia*
[3]*Centre for Quantum Dynamics, Griffith University, Nathan QLD 4111, Australia*
[4]*ARC Centre of Excellence for Quantum-Atom Optics, School of Mathematics and Physics, University of Queensland, St. Lucia QLD 4072, Australia*

(Received 1 December 2010; published 29 March 2011)

Proposals for long-distance quantum communication rely on the entanglement of matter-based quantum nodes through optical communications channels, but the entangling light pulses have poor temporal behavior in current experiments. Here we show that nonlinear mixing of a quantum light pulse with a spectrally tailored classical field can compress the quantum pulse by more than a factor of 100 and flexibly reshape its temporal waveform while preserving all quantum properties, including entanglement. Our scheme paves the way for quantum communication at the full data rate of optical telecommunications.

DOI: 10.1103/PhysRevLett.106.130501 PACS numbers: 03.67.Hk, 03.67.Ac, 42.50.−p, 42.65.Ky

The development of long-distance quantum communication is critical for future quantum cryptography and distributed quantum computing applications [1]. Current fiber-optical quantum communication systems rely on direct transmission of quantum light pulses, but the attenuation of the fiber imposes a distance limit of tens of kilometers for this kind of quantum communication [2] by virtue of the no-cloning theorem [3]. Quantum repeater architectures [4,5] promise to circumvent this limit by preparing entangled states over an optical communications channel and storing these entangled states as a resource for subsequent quantum communication. Components of quantum repeaters have now been demonstrated with a wide variety of physical systems, including single atoms [6,7], atomic vapors [8], rare-earth ions in solids [9], quantum dots [10], and nitrogen-vacancy centers [11]. The common thread among these demonstrations is the manipulation of quantum light pulses by matter-based quantum emitters. The temporal waveform of such emitters is typically a single-sided exponential with decay constant on the order of a few nanoseconds, while telecommunications networks are designed for smooth pulses with durations of tens of picoseconds [12]. Because of this mismatch, only a small fraction of the available telecommunications bandwidth is available for long-distance quantum communication. The magnitude of the difficulty is exemplified by a recent experiment which interfaced pulses of a record-breaking 1 ns duration with an atomic vapor [13]. These pulses are still 2 orders of magnitude longer than desired, and the nonresonant interaction technique used to increase the temporal bandwidth of the memory is not readily generalized to quantum systems other than atomic vapors. A recently proposed scheme for pulse compression in atomic vapor achieves compression by a factor of 10 at a fidelity of ~80% [14], and compression and reshaping of optical coherent states have been demonstrated with similar techniques in recent experiments [15].

Here we present an efficient and straightforward method of quantum optical pulse shaping and compression that simplifies the interfacing of quantum emitters with telecommunications networks. Compression by more than a factor of 100 and flexible reshaping of the temporal waveform can be achieved with errors below 1%. Our method preserves the full quantum statistics of the input field, including entanglement and any other multimode correlations. Spontaneously emitted photons from any type of quantum emitter can be converted to smooth pulses with tens of picoseconds duration at a specified wavelength, making them directly compatible with standard telecommunications technology [12] and allowing utilization of the full fiber-optical channel capacity for long-distance quantum communication.

The scheme for quantum optical waveform conversion is shown in Fig. 1. The input pulse undergoes three-wave mixing (3WM) with a frequency-chirped classical laser

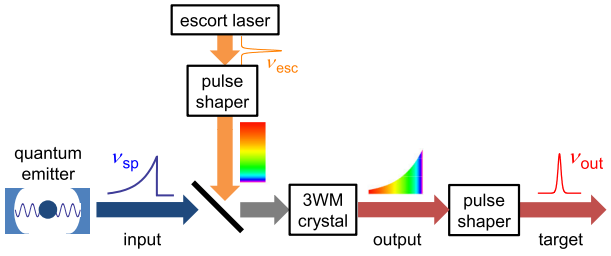

FIG. 1 (color online). Scheme for quantum optical waveform conversion. The colors under the pulse envelope accurately represent the frequency variation during the pulse length, with the variation of colors greatly exaggerated for clarity.

pulse. For an appropriate choice of classical laser intensity and chirp, the 3WM product radiation has the same spectrum as the desired target mode, but receives the quantum statistics of the input. The 3WM output is then dechirped with a second pulse shaper to match the temporal wave function of the target mode. The waveform conversion technique builds on recent experiments on temporal modulation of single-photon wave packets [16] and nonlinear frequency conversion with single photons [17], which show that nonlinear modulation and dispersion are compatible with preservation of quantum information in practice as well as in theory. Our technique can be regarded as an extension of the time lens, which has achieved remarkable results in compressing and stretching classical pulses [18], to the quantum domain and to arbitrary pulse reshaping. Waveform conversion can be readily implemented with present-day single-photon frequency conversion devices, upgrading them from simple wavelength converters to flexible interfaces for long-distance quantum communication.

We analyze the 3WM process using the canonical quantization method [19]. For simplicity, the electric field polarization vectors are assumed to lie along the 3WM crystal axes, as for a periodically poled or otherwise noncritically phase-matched crystal. We assume conservation of momentum and energy for the carrier waves and retain only phase-matched processes. The escort laser pulse contains $\gtrsim 10^{10}$ photons and can be approximated as a classical field that remains unaffected by 3WM. The input and output quantum fields are then described by slowly varying bosonic field operators $\Psi_j(z, t)$, with $j = 1$ the input mode and $j = 2$ the mode generated by 3WM. Here z measures the distance along the propagation axis in a frame comoving at the group velocity and t measures the duration of the interaction between the three fields [20]. The escort field is taken to be a classical field of constant intensity that is phase modulated to impart the desired spectral modulation to mode 2. We write $\Psi_3 = \xi \exp[i\phi(z)]$, where ξ is the (real, positive) amplitude of the classical escort field and $\phi(z)$ is the local phase. In the absence of dispersion, the 3WM Hamiltonian becomes

$$H_{\mathrm{3WM}} = i\hbar\Omega \int dz e^{i\phi(z)} \Psi_1^\dagger \Psi_2 + \mathrm{H.c.}, \tag{1}$$

where Ω is determined by the nonlinear coupling constant and the intensity of the escort pulse and can be computed by taking the classical limit of 3WM. The quantum field operators evolve as

$$\Psi_1(z, t) = \cos\Omega t \Psi_1(z, 0) + \sin\Omega t e^{i\phi(z)} \Psi_2(z, 0), \tag{2}$$

$$\Psi_2(z, t) = -\sin\Omega t e^{-i\phi(z)} \Psi_1(z, 0) + \cos\Omega t \Psi_2(z, 0). \tag{3}$$

If the fields leave the 3WM medium after an interaction time $T = \pi/(2\Omega)$, the solution for mode 2 at times $t > T$ is just $\Psi_2(z, T) = -e^{-i\phi(z)} \Psi_1(z, 0)$. The quantum state of mode 1 is perfectly transferred into mode 2, while mode 2 has acquired the phase $-\phi(z) + \pi$ from mode 3.

The required form of $\phi(z)$ can be derived by considering the classical limit of the input and output fields. We denote the (normalized) input temporal waveform by $\alpha_1(z)$ and the desired output waveform by $\alpha_2(z)$. To match the power spectrum of the 3WM product to the desired spectrum, $\phi(z)$ should satisfy $|\tilde{\alpha}_2(k)| \propto |\int dz \alpha_1(z) e^{i\phi(z)} e^{-ikz}|$, where $\tilde{f}(k)$ is the Fourier transform of $f(z)$. When the input and target bandwidths differ substantially, the method of stationary phase applies to the integral and $\phi(z)$ has a closed-form solution when the target is Gaussian, $\alpha_2(z) \propto e^{-z^2/(2\sigma^2)}$. After 3WM, the phase of $\tilde{\alpha}_2(k)$ is nontrivial and the 3WM product pulse is therefore not transform limited. The output pulse shaper then applies a spectral compensation phase $\gamma(k)$, implementing the unitary transformation

$$\Psi_{\mathrm{out}}(z) = \frac{1}{2\pi} \int dz' \Psi_2(z, t = T) \int dk e^{i\gamma(k)} e^{ik(\zeta - z')}. \tag{4}$$

Choosing $\gamma(k) = kz_0 - \phi(z_0)$, where z_0 is the solution to $\phi'(z_0) = k$, removes the unwanted phase. Then the output pulse is transform limited with the desired spectrum. When $\alpha_1(z) \propto e^{-z^2/(2\mu^2)}$ is also Gaussian, one finds $\phi(z) = \sigma z^2/(2\mu)$ and $\gamma(k) = -\mu k^2/(2\sigma)$, while for a single-sided exponential of decay time τ the solutions are

$$\phi(z) = \frac{\sqrt{2}}{\sigma} \int_0^z d\zeta^{-1} \,\mathrm{erf}^{-1}(e^{-\zeta/(c\tau)}), \tag{5}$$

$$\gamma(k) = -k \log \mathrm{erf} \frac{k\sigma}{\sqrt{2}} - \sigma\sqrt{\frac{2}{\pi}} \int_0^k d\kappa \frac{\kappa e^{-\kappa^2\sigma^2/2}}{\mathrm{erf}(\kappa\sigma/\sqrt{2})}. \tag{6}$$

The phase functions of Eqs. (5) and (6) are visualized in Fig. 2. $\gamma(k)$ can be applied using standard dispersive pulse shaping techniques [21] with, e.g., a liquid crystal phase mask or lithographically fabricated phase plate that makes a step approximation to the desired phase function. The escort phase $\phi(z)$ may be applied by, e.g., linearly chirping the escort pulse to the nanosecond domain and applying subsequent phase modulation with a high-bandwidth electro-optic modulator (EOM). A finite number of phase resolution elements N_{res} are available to approximate each phase function, determined for $\gamma(k)$ by the number of pixels in the phase mask and for $\phi(z)$ by the EOM bandwidth. We use the Nyquist criterion to estimate the range of

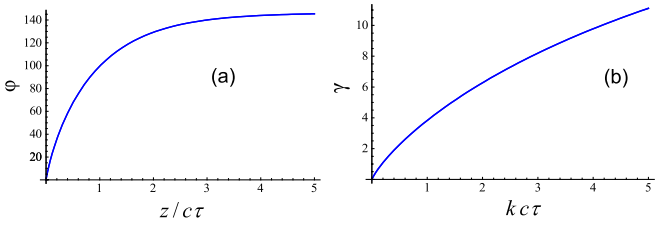

FIG. 2 (color online). (a) Escort phase modulation function $\phi(z)$ and (b) recompression phase modulation function $\gamma(k)$ for conversion from a single-sided exponential waveform to a Gaussian waveform with compression ratio $\tau/\sigma = 100$.

good approximation and calculate the associated approximation fidelity F_{approx} as the norm of the classical pulse shape over this range. For example, consider conversion of a single-sided exponential to a Gaussian at compression factor $\tau/\sigma = 100$. The most stringent constraint on the phase is found to occur for $\phi(z)$ at the rising edge of the exponential. For an experimentally reasonable EOM bandwidth of several GHz, $N_{\text{res}} = 1000$ over a window $0 < z/(c\tau) < 6$, yielding a phase approximation error of $1 - F_{\text{approx}} = 8.5 \times 10^{-3}$.

Dispersion in the 3WM medium is the fundamental source of error in the waveform conversion. The quantum Hamiltonian for group-velocity mismatch (GVM) and group-velocity dispersion (GVD) can be written as [22]

$$H_{\text{disp}} = \sum_{j=1,2} \int dz \left[\frac{i\hbar v_j}{2} \frac{\partial \Psi_j^\dagger}{\partial z} \Psi_j + \frac{\beta_j}{4} \frac{\partial \Psi_j^\dagger}{\partial z} \frac{\partial \Psi_j}{\partial z} \right] + \text{H.c.}, \tag{7}$$

where $v_{1,2,3}$ are the group velocities of the modes. The 3WM Hamiltonian (1) is also modified because the phase $\phi(z)$ of the escort field phase evolves under dispersion. Moving to the interaction picture with respect to the original 3WM Hamiltonian (1), one derives the additional unitary evolution due to dispersive effects, U_{disp} [23]. The GVM is conveniently parametrized by $v = (v_1 - v_2)/2$, $v_e = v_3 - (v_1 + v_2)/2$. The dispersive correction can be canceled to first order by adding a compensation phase

$$\Delta_{\text{opt}}(z) = \frac{\pi}{4\Omega}(v_e - v)\phi'(z) \tag{8}$$

to the initial escort phase $\phi(z)$. A second-order Dyson series solution for U_{disp} shows that GVM mixes the vacuum noise of the initially unoccupied mode 2 into the state transfer, while GVD has a negligible effect. The removal of phase by the output pulse shaper just implements a unitary transformation on the 3WM output field, which has no effect on the error.

We quantify the error in waveform conversion using the fidelity F. For pure input states, $F = |\langle \psi_{\text{ideal}} | \psi_{\text{disp}} \rangle|$, where the result of ideal evolution is written $|\psi_{\text{ideal}}\rangle$ and the result with dispersion included is $|\psi_{\text{disp}}\rangle$. If the input system is entangled with another quantum system, the fidelity of the final entangled state is simply the average fidelity of the eigenstates of the input density operator, weighted by their corresponding eigenvalues. The fidelity is then evaluated as $F = |\langle U_{\text{disp}} \rangle|$, where the expectation value is taken with respect to the initial states of modes 1 and 2 and any other systems entangled with mode 1. Compensating the phase according to Eq. (8) is found to minimize the error independently of the input state. We take mode 2 to be initially in a vacuum state, with mode 1 having an average photon number of $\langle n \rangle$ in a spatial wave function $A(z)$ with characteristic length scale L. Defining dimensionless velocities $u = v/v_0$, $u_e = v_e/v_0$, where $v_0 = \Omega L/(2\pi)$, we then obtain [23]

$$1 - F_{\text{opt}} = \frac{\langle n \rangle u^2 L^2}{32\pi^2} \int dz |2A'(z) - i(1 + u_e/u)\phi'(z)A(z)|^2. \tag{9}$$

The ratio u_e/u is set by the crystal dispersion alone, but u varies with the escort laser intensity I_{esc} as $u \propto I_{\text{esc}}^{-1/2}$. Thus the fidelity can be made arbitrarily close to 1 by increasing the escort laser power. Equation (9) can then be rewritten as $1 - F_{\text{opt}} = (u/u_{\text{err}})^2$ for some $u_{\text{err}} \lesssim 1$. It can be seen from Eq. (9) that the perturbation theory breaks down for a pulse with an arbitrarily sharp leading edge; a perturbative analysis in momentum space shows that $1 - F_{\text{opt}} \propto u$ in this limit. In practice, the time required to excite a quantum emitter is never exactly zero, so the leading edge of the pulse is smoothed over the excitation time scale.

To check the validity of the perturbative calculation, we also perform full numerical simulations of the waveform conversion process. The Heisenberg equations of motion for the field operators Ψ_1, Ψ_2 are linear, so the operator of the target field after time t will be a linear combination of the initial field operators. If the input pulse has a single spatial mode $A(z)$, such that $|\psi(0)\rangle = f[a^\dagger]|0\rangle = f[\int dz A(z)\Psi_1^\dagger(z)]|0\rangle = \sum_n c_n |n\rangle$, the quantum state at time t is

$$|\psi(0)\rangle = f\left[\int dz \{A_1(z,t)\Psi_1^\dagger(z) + A_2(z,t)\Psi_2^\dagger(z)\} \right]|0\rangle, \tag{10}$$

with $A_1(z,0) = A(z)$ and $A_2(z,0) = 0$. The A_n obey the same linear equations as Ψ_n, but are c-number amplitudes rather than operators. The fidelity can then be calculated as before. For fidelities close to unity and a correctly compensated phase, this procedure reproduces the linear dependence on $\langle n \rangle$ found in the perturbative calculation (9). For definiteness, we only show results for a single-photon input state. The results confirm that the effect of group-velocity dispersion is insignificant in all cases of interest.

The intrinsic error in waveform conversion due to dispersion in the 3WM medium can be less than 0.1% for readily achievable experimental parameters. Figure 3 shows the analytic and numerical error estimates for two cases of particular experimental interest. Case 1: the conversion of 370 nm photons from a Yb^+ ion [6] to the 1550 nm telecommunications band using periodically poled lithium niobate, for which $u_e/u \approx -2/3$. The exponential rise time is taken to be 0.02τ. The simulated error closely follows the perturbative result for small values of u up to a compression ratio $\tau/\sigma = 200$. For an escort laser pulse of energy ~ 1 μJ and duration of 150 ns ($> 20\tau_{Yb^+}$) in a 50 mm long crystal waveguide, one finds $u = 0.013$ and error of $1 - F = 7 \times 10^{-4}$ at compression ratio of 100. Case 2: the conversion of 780 nm photons from a

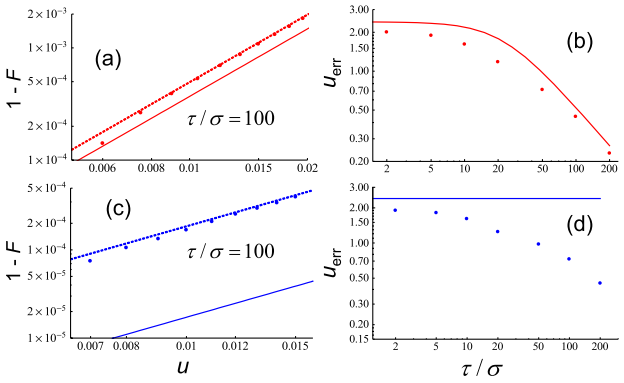

FIG. 3 (color online). Dispersive error induced by quantum waveform conversion. (a) Case 1 of the text. Solid line: perturbative prediction. Points: simulation results. Dashed line: best fit of $1 - F = (u/u_{\mathrm{err}})^2$ to simulation points. (b) Error scale u_{err} as a function of compression ratio τ/σ. Solid line: perturbative prediction. Points: simulated values computed from least-squares fits to simulation results. Panels (c) and (d) are the same as (a) and (b) but for case 2 of the text.

Rb atom to the telecommunications band, for which one can arrange $u_e/u = -1$ by poling lithium niobate for type II phase matching [24]. Errors are even lower than for conversion of 370 nm photons, but at compression ratio above 10 the perturbation theory breaks down and higher-order GVM dominates the error. $v < 10^5$ m/s for any choice of output wavelengths in the telecommunications band, so $u < 10^{-4}$ and $1 - F \ll 10^{-4}$.

We have shown that three-wave mixing with a modulated classical field can reshape and compress the waveform of a quantum light pulse while faithfully maintaining the quantum information carried by the photons. A quantum light pulse produced by a quantum emitter with a lifetime of nanoseconds can be converted to a Gaussian pulse with a duration of tens of picoseconds that is compatible with standard telecommunications protocols [12]. The low error of waveform conversion is compatible with schemes for fault-tolerant quantum communication over long distances [4]. Quantum waveform conversion enables simultaneous time- and wavelength-division multiplexing of the pulses from an array of quantum emitters up to the limit of channel capacity, massively increasing quantum communications bandwidth. Current telecommunications systems employ dense wavelength-division multiplexing (DWDM) with 50 GHz channel spacing and therefore achieve their maximum capacity for transform-limited pulses with ~20 ps duration, while the dispersive effects of long-haul fiber transmission require the pulses to have a smooth temporal waveform. As each pulse arrives from the emitter array, it can be simultaneously converted to this ideal waveform and sorted into an appropriate DWDM channel. The rate of entangled pair generation in a quantum network is then limited only by the telecommunications bandwidth and the size of the emitter array.

This work was supported by the Australian Research Council under DP0773354 (D. K.), CE0348250 and CE110001027 (H. M. W.), and CE0348178 (J. F. C.). We thank Geoff Pryde for helpful conversations.

[1] H. J. Kimble, Nature (London) **453**, 1023 (2008).
[2] N. Gisin, G. Ribordy, W. Tittel, and H. Zbinden, Rev. Mod. Phys. **74**, 145 (2002).
[3] W. K. Wootters and W. H. Zurek, Nature (London) **299**, 802 (1982).
[4] H.-J. Briegel, W. Dur, J. I. Cirac, and P. Zoller, Phys. Rev. Lett. **81**, 5932 (1998).
[5] L.-M. Duan, M. D. Lukin, J. I. Cirac, and P. Zoller, Nature (London) **414**, 413 (2001).
[6] B. B. Blinov, D. L. Moehring, L.-M. Duan, and C. Monroe, Nature (London) **428**, 153 (2004).
[7] J. McKeever *et al.*, Science **303**, 1992 (2004); M. Kellerit *et al.*, Nature (London) **431**, 1075 (2004).
[8] C. W. Chou, S. V. Polyakov, A. Kuzmich, and H. J. Kimble, Phys. Rev. Lett. **92**, 213601 (2004); B. Julsgaard *et al.*, Nature (London) **432**, 482 (2004); M. Hosseini *et al.*, Nature (London) **461**, 241 (2009).
[9] H. de Riedmatten *et al.*, Nature (London) **456**, 773 (2008); M. P. Hedges, J. J. Longdell, Y. Li, and M. J. Sellars, Nature (London) **465**, 1052 (2010).
[10] S. T. Yılmaz, P. Fallahi, and A. Imamoğlu, Phys. Rev. Lett. **105**, 033601 (2010).
[11] E. Togan *et al.*, Nature (London) **466**, 730 (2010).
[12] See International Telecommunications Union, ITU-T recommendations G.680 and G.698.1 at www.itu.int.
[13] K. F. Reim *et al.*, Nat. Photon. **4**, 218 (2010).
[14] S. A. Moiseev and W. Tittel, Phys. Rev. A **82**, 012309 (2010).
[15] M. Hosseini *et al.*, Nature (London) **461**, 241 (2009); B. C. Buchler *et al.*, Opt. Lett. **35**, 1091 (2010).
[16] H. P. Specht *et al.*, Nat. Photon. **3**, 469 (2009); C. Belthangady *et al.*, Phys. Rev. Lett. **104**, 223601 (2010).
[17] A. P. Vandevender and P. G. Kwiat, J. Mod. Opt. **51**, 1433 (2004); M. A. Albota and F. N. C. Wong, Opt. Lett. **29**, 1449 (2004); C. Langrock *et al.*, Opt. Lett. **30**, 1725 (2005); S. Tanzilli *et al.*, Nature (London) **437**, 116 (2005); M. T. Rakher *et al.*, Nat. Photon. **4**, 786 (2010).
[18] C. V. Bennett and B. H. Kolner, Opt. Lett. **24**, 783 (1999); M. A. Foster *et al.*, Nat. Photon. **3**, 581 (2009).
[19] M. Hillery and L. D. Mlodinow, Phys. Rev. A **30**, 1860 (1984); P. D. Drummond, Phys. Rev. A **42**, 6845 (1990); M. Hillery, Acta Phys. Slovaca **59**, 1 (2009).
[20] This coordinate convention is to be contrasted with the classical nonlinear optics convention in which z measures the interaction length in the 3WM medium and t is the time of arrival at the detector.
[21] A. M. Weiner, Rev. Sci. Instrum. **71**, 1929 (2000).
[22] P. D. Drummond and J. F. Corney, J. Opt. Soc. Am. B **18**, 139 (2001).
[23] See supplemental material at http://link.aps.org/supplemental/10.1103/PhysRevLett.106.130501 for details of the perturbative calculation of error in waveform conversion.
[24] N. E. Yu *et al.*, Opt. Lett. **27**, 1046 (2002).